Forsch Ingenieurwes (2007) 71: 69–78
DOI 10.1007/s10010-006-0044-2

ORIGINALARBEITEN · ORIGINALS

Determination of local heat transfer coefficient from the solution of the inverse heat conduction problem

J. Taler

Received: 20 November 2006 / Published online: 6 February 2007

Abstract The aim of this paper is to present two techniques for simply and accurately determining space-variable heat transfer coefficient, given measurements of temperature at some interior points in the body. The fluid temperature is also measured as part of the solution. The methods are formulated as linear and non-linear least-squares problems. The unknown parameters associated with the solution of the inverse heat conduction problem (IHCP) are selected to achieve the closest agreement in a least squares sense between the computed and measured temperatures using the Levenberg–Marquardt method (method I) or the singular value decomposition (method II). The methods presented in the paper are used for determining the local heat transfer coefficient on the circumference of the vertical smooth tube placed in the tube bundle with a staggered tube arrangement. Good agreement between the results is obtained. The uncertainties in the estimated heat transfer coefficients are calculated using the error propagation rule of Gauss. The main advantage of the presented methods is that they do not require any complex simulation of flow and temperature field in the fluid.

Ermittlung des örtlichen Wärmeübergangskoeffizienten aus der Lösung des inversen Wärmeleitungsproblems

Zusammenfassung In der Arbeit wurden zwei Verfahren zur einfachen und genauen Bestimmung des lokalen Wärmeübergangskoeffizienten auf der Basis der in inneren Punkten des Körpers gemessenen Temperaturen entwickelt. Die Umgebungstemperatur wird auch gemessen. Das erste Verfahren wird als lineare und das zweite Verfahren als nichtlineare Aufgabe der kleinsten Quadrate formuliert. Die unbekannten Parameter, die in dem inversen Problem der Wärmeleitung auftreten, werden so gewählt, daß die beste Übereinstimmung zwischen den berechneten und gemessenen Temperaturen erzielt wird. Zur Bestimmung der unbekannten Parameter wurden zwei Methoden angewandt: das Verfahren von Levenberg–Marquardt (Methode I) und die singuläre Matrix-Zerlegung (Methode II). Die entwickelten Methoden wurden zur Bestimmung des örtlichen Wärmeübergangskoeffizienten an der außen Oberfläche des Rohres, das sich in der Bündel mit der versetzten Rohranordnung befindet, angewandt. Die Unsicherheiten in den ermittelten Wärmeübergangskoeffizienten wurden nach dem Gaußschen Prinzip der Fehler Fortpflanzung berechnet. Eine numerische Simulation des Temperatur- und Strömungsfeldes im Fluidgebiet ist nicht notwendig, was der Hauptvorteil der beiden Methoden ist.

List of Symbols

f_i	measured temperature, °C
h	heat transfer coefficient, W/(m^2 K)
H	tube height, m
$\boldsymbol{I_n}$	identity matrix
$\boldsymbol{J_m}$	Jakobian matrix
k	thermal conductivity, W/(m K)
m	number of measurement points
n	number of unknown parameters
$\dot{q}$	heat flux, W/m^2
$\dot{Q}$	heat flow rate, W
r	radius, m
s_i	singular value
S	sum of squares, K^2
T	temperature, °C

J. Taler (✉)
Institute for Process and Power Engineering,
Cracow University of Technology,
31-864 Kraków, Poland
e-mail: taler@ss5.mech.pk.edu.pl

T_i calculated temperature, °C
$\boldsymbol{x}$ vector of unknown parameters

Greek symbols

φ angle measured from the stagnation point on the inflow tube side, rad
σ standard deviation

Subscripts

h heated surface
in inner
m measured
o outer
∞ fluid

1 Introduction

Local convective heat transfer coefficient can be measured by a variety of different methods. Mass transfer methods are widely used since many years [1–4]. The heat-mass transfer analogy, in conjunction with the naphthalene sublimation technique, was used to investigate local and average heat transfer coefficients in two-row plate fin and tube heat exchanger with circular tubes [1]. The local mass transfer coefficients on this geometry have also been measured by Krückels and Kottke [3]. They used a chemical method based on absorption, chemical reaction and coupled colour reaction [4]. The solid surface is coated with a wet filter paper and ammonia to be transferred is added as a short gas pulse. The locally transferred mass is visible as colour density distribution and the colour intensity corresponds to the local mass (heat) flow.

Thermochromic liquid crystals have been applied extensively to heat transfer measurements [4–7]. Using temperature maps obtained from liquid crystals applied to a constant heat flux surface, the Newton's Law of Cooling (the boundary condition of the third kind) is used to establish distributions of the convective heat transfer coefficient. A constant heat flux at the body surface is typically generated by passing an electrical current through a fin film with uniform electrical resistivity.

Thermographic phosphors have also been used for local heat transfer measurements [8, 9]. Application of temperature sensitive paints to heat transfer measurements are described by Liu and Sullivan [10].

Optical measurement techniques have found widespread application in heat transfer investigations [7, 11, 12]. Differential interferometry can be used to determine local temperature gradients in the fluid and a local heat transfer coefficient at the solid surface.

However, these methods either require expensive experimental equipment or have limited application to high temperatures. An alternative method to obtain the local convective heat coefficient, that feasible for examination of objects at high temperature, is the inverse heat conduction technique.

The purpose of this study is to use a solution of an inverse heat conduction problem for measuring the distribution of convective local heat transfer coefficients on the surface of a body. One advantage of this method is that measurements can be carried out with simple, low cost experimental models and equipment.

The determination of the distribution of the heat transfer coefficient on the surface of cylinders immersed in transversal flow of a fluid has been the subject of many papers [13–18] for many years. The values of the local heat transfer coefficient are necessary to determine the maximum temperatures of structural elements, e.g. of superheater tubes or fibers of hot-wire anemometers. Experimental determination of the local heat transfer coefficient on the surface of a cylinder or tube is very difficult in view of the small difference between the surface temperature of the cylinder which is immersed in cross flow and the liquid, and considering the high circumferential heat flow in the tube or cylinder wall. The occurrence of a circumferential heat flow impedes calculating the heat flow density $\dot{q}_o$ (on the outer surface of a tube or hollow cylinder with r_o radius) from an experimentally known flux density $\dot{q}_{in}$ on the internal surface (with radius r_{in}) using the simple relation, $\dot{q}_o r_o = \dot{q}_{in} r_{in}$, which is valid only for one dimensional temperature fields.

New experimental techniques, as well as new algorithms to solve inverse problems enabling determination of the local heat transfer coefficient are still being elaborated. In spite of many efforts of theorists and experimentalists, they did not achieve a simple and accurate method to determine $h(\varphi)$, where φ denotes the angle measured from the stagnation point on the liquid inflow side.

In inverse algorithms, being very sensitive even to minor temperature measurement inaccuracies, postulations are often assumed, which are hard to be implemented in practice, e.g. that the measurement points shall lay exactly in the nodes of the control volumes grid, or that an excessive number of temperature measurement points should be assumed, disturbing the temperature field to be identified.

The disadvantage of experimental techniques consists in the simplified theoretical analysis [13, 14].

Figure 1 presents some constructions of test cylinders, which can be applied to determine the local heat transfer coefficient.

The heat flux is generated in the center of the cylinder (Fig. 1a) or tube (Fig. 1b) by an electric heating element. A tube can also be heated by means of heating foils glued to the internal surface (Fig. 1c) or external surface (Fig. 1d) of the tube. If the temperature distribution in the cross-section of a tube or cylinder is to be determined by solving the in-

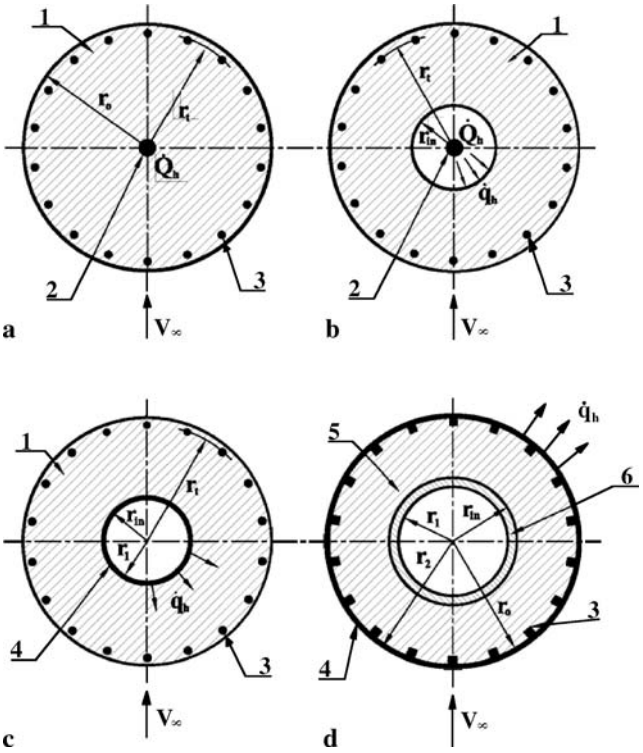

Fig. 1 Location of heating elements and thermocouples in tubes and cylinders in transversal air flow; 1 – tube or cylinder, 2 – heating element, 3 – thermocouple, 4 – heating foil, 5 – foamed polystyrene, 6 – PVC tube

verse heat conduction problem, then the thermocouples used to measure the wall temperature should be located close to the external surface (Figs. 1a–c), in order to avoid ill conditioning of the inverse problem.

Solving the inverse problem is avoided when applying the heating foil on the external tube surface. The foil temperature is measured by means of thermocouples placed in grooves made in the external surface of a phenolic resin tube with small wall thickness.

In the inside of the phenolic resin tube there is a foamed polystyrene tube with low thermal conductivity. In view of the small thickness of the Inconel 600 heating foil, amounting of 25 μm, the circumferential heat flow can be neglected [14].

When measuring the local heat transfer coefficient on a single tube placed in transversal air flow, the number of thermocouples under the foil can be small as the cylinder can be rotated about its axis by a small angle during the measurements [14].

While there have been many studies on local forced heat transfer from a single cylinder to air, there have been few such studies for cylinders placed in the tube bundle. With known uniform heat flux at the inner surface of the tube placed in the tube array, heat flows by conduction not only in radial but also in the circumferential direction due to the asymmetric nature of the air flow around the perimeter of the tube so that it is impossible to calculate heat flux on the outer tube surface from the one dimensional relation.

The circumferential heat flow affects the wall temperature distribution to such an extent that the heat flux at the outer tube surface is highly non-uniform. The temperature of the tube is measured at seven locations on the outer half of the tube circumference using K-type sheathed thermocouples of 1 mm in diameter placed at the distance of 0.5 mm from the outer tube surface. The heat flux $\dot{q}_h$ on the inner surface of the tube is calculated based on the measured electric power of the resistance heater placed inside the tube. The temperature distribution on the entire tube cross-section and heat flux distribution on the outer tube surface will be determined from the solution of the inverse heat conduction problem. The heat flux at the inner surface, $\dot{q}_h$, fluid temperature, T_∞, thermal conductivity of tube wall material, k, and measured tube wall temperatures f_i are the input data for solving inverse heat conduction problem.

Two methods presented in the paper will be used to solve the IHCP problem and to determine the local heat transfer coefficient around the tube periphery.

In the first method, the problem of determining space-variable heat transfer coefficient is formulated as a non-linear parameter estimation problem by approximating the distribution of the heat transfer coefficient on the boundary by the trigonometric Fourier polynomial. The unknown Fourier coefficients are estimated by the Levenberg–Marquardt method. The finite volume method [19] is used for solving direct heat conduction problem at each iteration step.

Linearization of the least-squares problem in the second method is accomplished by approximating unknown temperature on the boundary using the Fourier polynomial. The coefficients of the Fourier polynomial are the parameters to be estimated. The temperature distribution in the studied domain is determined by the method of separation of variables. After the IHCP is solved, the distributions of the boundary heat flux and heat transfer coefficients are evaluated using the Fourier and the Newton Law of Cooling, respectively.

2 Formulating the inverse problem

The temperature field $T(r, \varphi)$ in the cross-section of a tube or hollow cylinder is described by the heat conduction equation

$$\frac{\partial^2 T}{\partial r^2} + \frac{1}{r}\frac{\partial T}{\partial r} + \frac{1}{r^2}\frac{\partial^2 T}{\partial \varphi^2} = 0 \tag{1}$$

and the boundary condition on the internal surface (Figs. 1a–c)

$$-k \left.\frac{\partial T}{\partial r}\right|_{r=r_{in}} = \dot{q}_h \,. \tag{2}$$

The boundary condition on the outer surface of the tube $r = r_o$ is unknown. Determining the temperature field in the whole analyzed area including the external surface is made possible due to temperature measurements at m internal points (r_i, φ_i)

$$T(r_i, \varphi_i) = f_i \,, \quad i = 1, \ldots, m \,, \quad m \geq n \,. \tag{3}$$

The following nomenclature is assumed in the Eqs. 1–3: T – temperature in °C, r – radius in m, r_{in} – internal radius in m, φ – angle measured from the stagnation point on the inflow side in rad, k – thermal conductivity in W/(mK), f_i – temperature measured at the point (r_i, φ_i) in °C, m – number of temperature measurement points, n – number of searched parameters.

In the following two methods are presented for determining the local heat transfer coefficient $h(\varphi)$, using the above formulated inverse problem.

In both methods the unknown parameters $x = (x_1, \ldots, x_n)^T$ are determined by minimizing sum of squares

$$S = (\boldsymbol{f} - \boldsymbol{T_m})^T (\boldsymbol{f} - \boldsymbol{T_m}) \,, \tag{4}$$

where $\boldsymbol{f} = (f_1, \ldots, f_m)^T$ is the vector of measured temperatures, and $\boldsymbol{T_m} = (T_1, \ldots, T_m)^T$ the vector of computed temperatures $T_i = T(r_i \varphi_i)$, $i = 1, \ldots, m$.

3 Method I – Solving the non-linear problem of least squares by the Levenberg–Marquardt method

The heat transfer coefficient on the circumference of the tube can be approximated by the function

$$h(\varphi) = h(\varphi, \boldsymbol{x}) = \sum_{i=1}^{n} x_i \cos[(i-1)\varphi] \,. \tag{5}$$

The boundary condition on the external tube surface has the form

$$-k \left.\frac{\partial T}{\partial r}\right|_{r=r_o} = h(\varphi) \left(T|_{r=r_o} - T_\infty \right) \,, \tag{6}$$

where T_∞ denotes the temperature of the medium in °C, and $h(\varphi)$ is given by Eq. 5. The parameters $x_1, \ldots, x_n$ will be determined by using the Levenberg–Marquardt method [20] so that the Eq. 4 is minimum. The parameters, $\boldsymbol{x}$, are determined by the following iteration

$$\boldsymbol{x}^{(k+1)} = \boldsymbol{x}^{(k)} + \delta^{(k)} \,, \quad k = 0, 1, \ldots \tag{7}$$

where

$$\delta^{(k)} = \left[\left(\boldsymbol{J}_m^{(k)}\right)^T \boldsymbol{J}_m^{(k)} + \mu^{(k)} \boldsymbol{I}_n \right]^{-1} \left(\boldsymbol{J}_m^{(k)}\right)^T \left[\boldsymbol{f} - \boldsymbol{T}_m \left(\boldsymbol{x}^{(k)}\right) \right] \,. \tag{8}$$

The Jacobian $\boldsymbol{J}_m$ is determined by the equation

$$\boldsymbol{J}_m = \frac{\partial T_m(\boldsymbol{x})}{\partial \boldsymbol{x}^T} = \left[\left(\frac{\partial T_i(\boldsymbol{x})}{\partial x_j} \right) \right]_{m \times n} \quad i = 1, \ldots, m \quad j = 1, \ldots, n \,. \tag{9}$$

The symbol $\boldsymbol{I}_n$ denotes the identity matrix of $n \times n$ dimension, and $\mu^{(k)}$ the weight coefficient, which changes in accordance with the algorithm suggested by Levenberg and Marquardt. The upper index T denotes the transposed matrix. Temperature distribution $T(r, \varphi, \boldsymbol{x}^{(k)})$ is computed at each iteration step by the control volume method. The system of algebraic equations for the temperatures in the nodes of control volumes is solved by the Gauss–Seidel method. The division of the tube cross section into $4(N+1)$ control volumes is shown in Fig. 2.

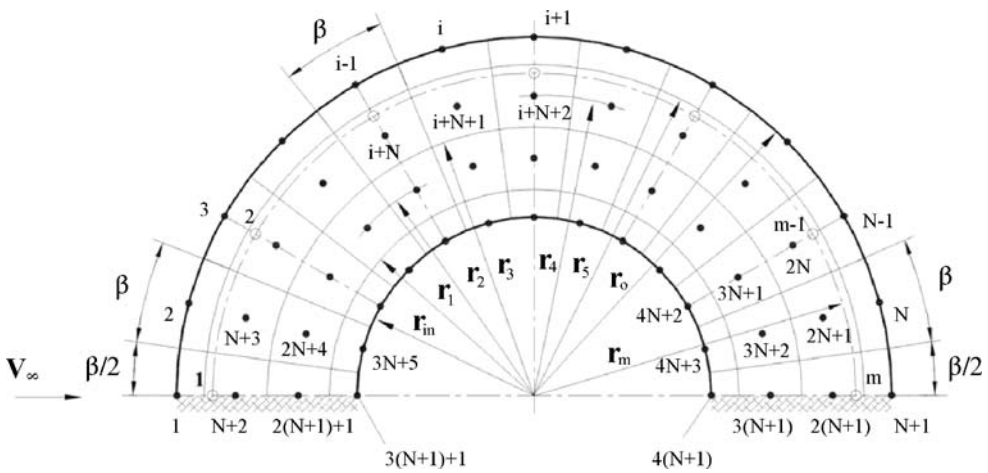

Fig. 2 Segmentation of a half tube cross-section into control volumes; • – nodes of control volumes, ○ – temperature measurement points

4 Method II – Solving the linear problem of least squares by matrix decomposition according to singular values

The second method is based on the singular value decomposition method (SVD) [21] that is used to find the least-squares solution to an over-determined set of linear algebraic equations. SVD is a very powerful method for dealing with sets of equations that may be singular, as in the case of inverse heat conduction problems which are very often ill-conditioned. The SVD technique will diagnose what the problem is: well-conditioned or ill-conditioned.

The method aims at finding the temperature distribution on the outer surface of a hollow cylinder or tube $T_o = T(r_o, \varphi)$, which is being approximated by the trigonometric polynomial

$$T|_{r=r_o} = \sum_{i=1}^{n} x_i \cos\left[(i-1)\,\varphi\right] = x_1 + \sum_{i=2}^{n} x_i \cos\left[(i-1)\,\varphi\right]. \tag{10}$$

The solution of the boundary problem (1, 2, 10) has the form

$$T\,(r,\varphi) = x_1 + \frac{\dot{q}_h\, r_{in}}{k} \ln\frac{r_o}{r} + \sum_{i=1}^{n} \left(\frac{r_{in}}{r_o}\right)^i \frac{x_{i+1}}{1+\left(\frac{r_{in}}{r_o}\right)^{2i}} \left[\left(\frac{r}{r_{in}}\right)^i + \left(\frac{r_{in}}{r}\right)^i\right] \cos\left(i\varphi\right), \tag{11}$$

where the heat flux density on the internal surface $r = r_{in}$ is computed by the formula $\dot{q}_h = \dot{Q}_h/(2\pi r_{in} H)$.

The symbols $\dot{Q}_h$ and H denote the power of the heater and the height of the examined tube. The expression 11 describing the temperature distribution can be written in the form

$$y\,(r,\varphi) = T\,(r,\varphi) - \frac{\dot{q}_h r_{in}}{k} \ln\frac{r_o}{r} = \sum_{i=1}^{n} x_i\, \phi_i\,(r,\varphi)\,, \tag{12}$$

where $\phi_1 = 1$, and $\phi_i\,(r,\varphi)$ for $i = 2, 3\ldots$ is given by the expression

$$\phi_i = \phi\,(r_i,\varphi_i) = \left(\frac{r_{in}}{r_o}\right)^i \frac{x_{i+1}}{1+\left(\frac{r_{in}}{r_o}\right)^{2i}} \left[\left(\frac{r}{r_{in}}\right)^i + \left(\frac{r_{in}}{r}\right)^i\right] \cos\left(i\varphi\right), \quad i = 2, 3, \ldots, n\,. \tag{13}$$

The over-determined system of equations in respect to $x_i\,, \quad i = 1, \ldots, n$

$$f_j - \frac{\dot{q}_h\, r_{in}}{k} \ln\frac{r_o}{r_j} - y_j \cong 0, \quad j = 1, \ldots, m \tag{14}$$

is solved using the matrix of coefficients $\boldsymbol{A}$ with singular values $s_1, \ldots, s_n$ .The system of Eq. 14 can be written in the form

$$\boldsymbol{A}\,\boldsymbol{x} \cong \boldsymbol{b}, \tag{15}$$

where $\boldsymbol{A}$ is a matrix of $m \times n$ dimension, the elements a_{jk} of which are expressed by n basis functions ϕ_i calculated at m points, i.e.: $a_{jk} = \phi_k\left(r_j, \varphi_j\right), \quad j = 1, \ldots, m, \quad k = 1, \ldots, n$.

The matrix $\boldsymbol{A}$ and the vector $\boldsymbol{b}$ have the form

$$\boldsymbol{A} = \begin{bmatrix} 1 & \phi_2\,(r_1\varphi_1) & \ldots & \phi_n\,(r_1\varphi_1) \\ 1 & \phi_2\,(r_2\varphi_2) & \ldots & \phi_n\,(r_2\varphi_2) \\ \ldots & \ldots & \ldots & \ldots \\ \ldots & \ldots & \ldots & \ldots \\ \ldots & \ldots & \ldots & \ldots \\ 1 & \phi_2\,(r_m\varphi_m) & \ldots & \phi_n\,(r_m\varphi_m) \end{bmatrix}_{m\times n}, \quad \boldsymbol{b} = \begin{bmatrix} f_1 - \frac{\dot{q}_h r_{in}}{k} \ln\frac{r_o}{r_1} \\ \ldots \\ \ldots \\ \ldots \\ \ldots \\ f_m - \frac{\dot{q}_h r_{in}}{k} \ln\frac{r_o}{r_m} \end{bmatrix}_m \tag{16}$$

The matrix of coefficients $\boldsymbol{A}$ of $m \times n$ size is being decomposed according to singular values [20]

$$\boldsymbol{A} = \boldsymbol{U} \cdot \boldsymbol{S} \cdot \boldsymbol{V}^T, \tag{17}$$

where $\boldsymbol{U}$ is an orthogonal matrix of $m \times n$ size, $\boldsymbol{S}$ – a diagonal matrix of singular values of $n \times n$ size with positive or zero singular values $s_1, \ldots, s_n$, and $\boldsymbol{V}$ – an orthogonal matrix of $n \times n$ size.

The solution of the over-determined set of Eq. 15 has the form

$$\boldsymbol{x} = \boldsymbol{V} \cdot \boldsymbol{S}^{-1} \cdot \left(\boldsymbol{U}^T \cdot \boldsymbol{b}\right) \tag{18}$$

When the singular value s_i equals zero, then in the inverse matrix $\boldsymbol{S}^{-1}$ it is to be assumed that $1/s_i$ also equals zero.

Upon determining the coefficients $\boldsymbol{x} = (x_1, \ldots, x_n)^T$ from Eq. 18 it is possible to determine the temperature distribution on the entire cross-section, while the heat flux density can be determined using the Fourier law as follows

$$\dot{q} = \dot{q}\,(r,\varphi) = -k\frac{\partial\, T\,(r,\varphi)}{\partial\, r} = \frac{\dot{q}_h r_{in}}{r} - \frac{k}{r} \sum_{i=1}^{n} \frac{i\, x_{i+1}}{1+\left(\frac{r_{in}}{r_o}\right)^{2i}} \left[1 - \left(\frac{r_{in}}{r}\right)^{2i}\right] \cos\left(i\varphi\right). \tag{19}$$

The heat transfer coefficient on the external surface of the tube following Newton's law is

$$h\,(\varphi) = \frac{\dot{q}\,(r_o,\varphi)}{\left[T\,(r_o,\varphi) - T_\infty\right]}\,. \tag{20}$$

The advantage of the method II is the very short computation time, as both the determination of the temperature field and of the parameters $x_1, \ldots, x_n$ do not require iteration. Method II can also be easily modified in order to account for the dependence of the thermal conductivity k on temperature.

5 The uncertainty of the results

The uncertainties of the determined parameters $\boldsymbol{x}$ and heat transfer coefficient $h(\varphi)$ were obtained using the error propagation rule of Gauss [20, 22]. The propagation of uncertainty in the independent variables: measured wall temperatures $f_1, \ldots, f_7$, thermal conductivity k and air temperature T_∞ is estimated from the following equation

$$2\sigma_{x_i} = \left[\sum_{j=1}^{7} \left(\frac{\partial x_i}{\partial f_j} 2\sigma_{f_j} \right)^2 + \left(\frac{\partial x_i}{\partial k} 2\sigma_k \right)^2 + \left(\frac{\partial x_i}{\partial T_\infty} 2\sigma_{T_\infty} \right)^2 + \left(\frac{\partial x_i}{\partial r_j} 2\sigma_{r_j} \right)^2 + \left(\frac{\partial x_i}{\partial \varphi_j} 2\sigma_{\varphi_j} \right)^2 \right]^{1/2}, \quad i = 1, 2, 3 \tag{21}$$

The uncertainty in the calculated heat transfer coefficient $h_k = h(\varphi_k)$ is determined in similar manner

$$2\sigma_{h(\varphi_k)} = \left[\begin{array}{l} \sum\limits_{j=1}^{7} \left(\frac{\partial h(\varphi_k)}{\partial f_j} 2\sigma_{f_j} \right)^2 + \left(\frac{\partial h(\varphi_k)}{\partial k} 2\sigma_k \right)^2 \\ + \left(\frac{\partial h(\varphi_k)}{\partial T_\infty} 2\sigma_{T_\infty} \right)^2 + \left(\frac{\partial h(\varphi_k)}{\partial r_j} 2\sigma_{r_j} \right)^2 \\ + \left(\frac{\partial h(\varphi_k)}{\partial \varphi_j} 2\sigma_{\varphi_j} \right)^2 \end{array} \right]^{1/2}, \quad k = 1, 2, \tag{22}$$

where φ_k is an angle from the interval: $0° \leq \varphi_k \leq 180°$. The 95% uncertainty in the estimated parameters can be expressed in the form of a bilateral tolerance using 95% limits as

$$\begin{aligned} x_i &= x_i^* \pm 2\sigma_{x_i}, \\ h(\varphi_k) &= h^*(\varphi_k) \pm 2\sigma_{h(\varphi_k)}, \end{aligned} \tag{23}$$

where x_i^*, $i = 1, 2, 3$ and $h^*(\varphi_k)$, $k = 1, 2, \ldots$ represent the value of the parameters and heat transfer coefficients obtained using the least squares method.

The sensitivity coefficients $\partial x_i / \partial f_j$, $\partial x_i / \partial k$, $\partial x_i / \partial T_\infty$, $\partial x_i / \partial r_j$, and $\partial x_i / \partial \varphi_j$ in the expression 22 and the coefficients $\partial h(\varphi_k) / \partial f_j$, $\partial h(\varphi_k) / \partial k$, $\partial h(\varphi_k) / \partial T_\infty$, $\partial h(\varphi_k) / \partial r_j$, and $\partial h(\varphi_k) / \partial \varphi_j$ in Eq. 22 were calculated by means of the numerical approximation using central difference quotients.

6 Example of determination of the local heat transfer coefficient

First numerical experiment with simulated data is presented. Consider a steel tube with the following parameters:

- outside diameter – $d_o = 25.0$ mm,
- inside diameter – $d_{in} = 19.8$ mm,
- thermal conductivity of the tube material (carbon steel) – $k = 53\ \mathrm{W/(mK)}$.

Because of the symmetry, only a half of the tube was considered. The tube wall temperature is measured by thermocouples located every 30° at 0.5 mm distance from the outer tube surface ($r_i = r_m = 12$ mm, $i = 1, \ldots, 7$). The positions of thermocouples are assumed to be known exactly. The air temperature is $T_\infty = 22.17\,°\mathrm{C}$. The boundary conditions at inner and outer surfaces are assumed to be known. The heat flux at the inner surface is $\dot{q}_h = 5293.91\ \mathrm{W/m^2}$, and the local heat transfer coefficient $h(\varphi)$ is given by

$$h(\varphi) = 165.133 + 108.46\cos(\varphi) + 123.76\cos(2\varphi), \tag{24}$$

where φ is the angle from the forward stagnation point. Then, the measured data were artificially generated using the commercial codes: FLUENT and ANSYS. A finite element mesh used with an ANSYS computation is shown in Fig. 3.

The temperature distribution in the tube cross section is shown in Fig. 4. The same "measured" values of the temperature were obtained using FLUENT: $f_1 = 45.54\,°\mathrm{C}$, $f_2 = 46.22\,°\mathrm{C}$, $f_3 = 47.84\,°\mathrm{C}$, $f_4 = 49.42\,°\mathrm{C}$, $f_5 = 50.22\,°\mathrm{C}$, $f_6 = 50.26\,°\mathrm{C}$, $f_7 = 50.17\,°\mathrm{C}$. The inverse analysis is then conducted to show the accuracy of the methods presented in the paper.

The unknown heat transfer coefficient in the first method and the unknown surface temperature in the second method were approximated by the polynomial of the third degree. The accuracy of the proposed method is assessed by comparing the estimated results with the input (exact) distribution of the heat transfer coefficient.

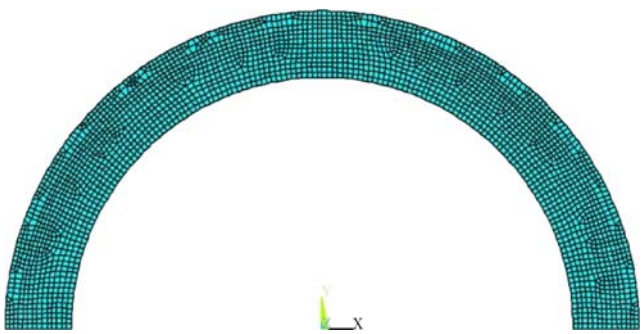

Fig. 3 Finite element mesh

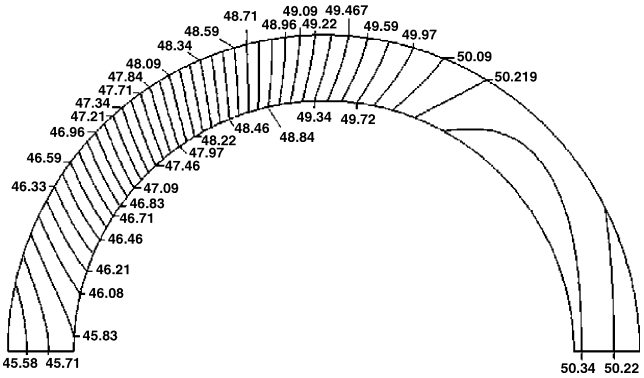

Fig. 4 Temperature distribution in °C in the tube cross section obtained by using ANSYS code

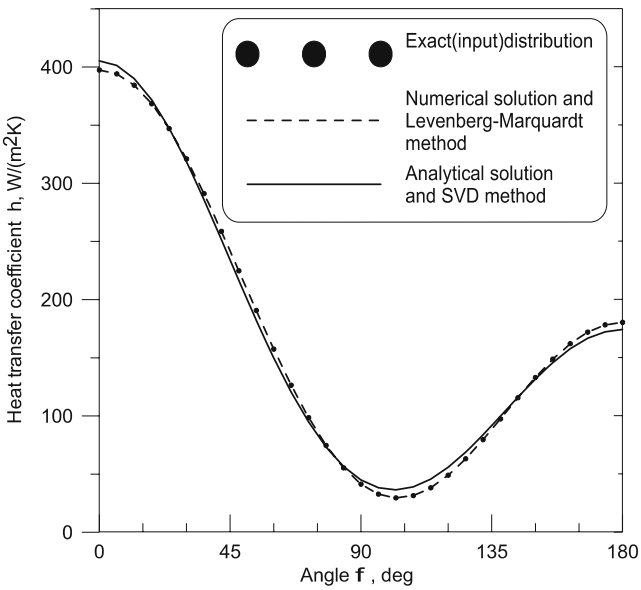

Fig. 5 Comparison of heat transfer coefficient $h(\varphi)$ on the tube half circumference determined by the presented methods with input distribution

The estimated results are shown in Fig. 5. The agreement between the known input distribution of the heat transfer coefficient and the inverse solutions is very good.

Both methods were applied to determine the distribution of the heat transfer coefficient on the circumference of a tube situated at the center of the fourth row of a bundle with staggered tube arrangement (Fig. 6).

A bundle of 36 tubes of length $H = 0.3\,\mathrm{m}$, internally heated by electric heater elements, is placed in a rectangular channel of $0.25 \times 0.3\,\mathrm{m}$ size. The pitches of the arrangement of tubes made of K18 steel with external diameter $d_o = 0.025\,\mathrm{m}$ and internal diameter $d_{in} = 0.0198\,\mathrm{m}$, are: $s_1 = 0.05325\,\mathrm{m}$ and $s_2 = 0.031\,\mathrm{m}$ (Fig. 6). The tube wall temperature was measured by sheathed thermocouples NiCr−Ni located every 30° at 0.5 mm distance from

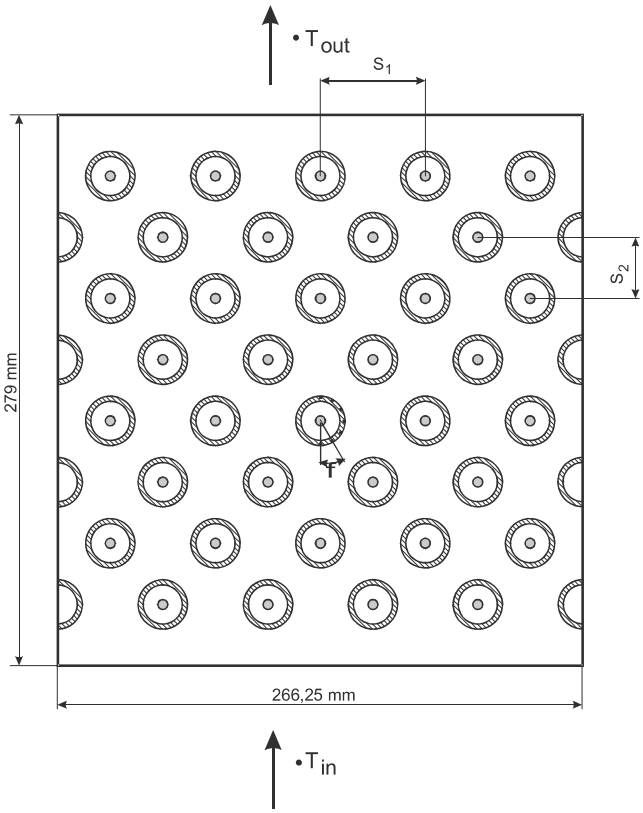

Fig. 6 Layout of the investigated bundle with staggered tube arrangement

the external tube surface ($r_i = r_m = 0.012\,\mathrm{m}$, $i = 1, \ldots, 7$, $m = 7$). The thermal conductivity of the material of the tubes is $k = 53\,\mathrm{W/(mK)}$. The temperature was measured when the heater power was $\dot{Q}_h = 112.8\,\mathrm{W}$ and the Reynolds number equaled $\mathrm{Re} = w_{\max} d_o/\nu = 11\,775\,\mathrm{m}$ where $w_{\max}$ is the air velocity in the narrowest cross section, d_o – the outer tube diameter, and ν – the kinematic viscosity of air. The air temperature was $T_\infty = 30.49\,^\circ\mathrm{C}$, and the wall temperatures at seven points located on the half of the tube were: $f_1 = 105.0\,^\circ\mathrm{C}$, $f_2 = 105.8\,^\circ\mathrm{C}$, $f_3 = 107.6\,^\circ\mathrm{C}$, $f_4 = 110.5\,^\circ\mathrm{C}$, $f_5 = 113.8\,^\circ\mathrm{C}$, $f_6 = 113.7\,^\circ\mathrm{C}$ and $f_7 = 112.7\,^\circ\mathrm{C}$. The temperature measurement points are numbered starting from the inflow side, i.e. the first thermocouple was situated at the point $(r_m, 0^\circ)$ and the seventh thermocouple at the point $(r_m, 180^\circ)$.

In order to show the influence of the measurement errors on the determined distributions of the heat transfer coefficients, the 95% confidence intervals were calculated. The following uncertainties of the measured values were assumed (at a 95% confidence interval):

$$\Delta f_j = \pm 0.1\,\mathrm{K}, \quad j = 1, \ldots, 7, \quad \Delta T_\infty = \pm 0.1\,\mathrm{K},$$
$$\Delta \dot{Q}_h = \pm 0,01\,\dot{Q}_h, \quad \Delta k = \pm 0.5\,\mathrm{W/(mK)},$$
$$\Delta r_j = \pm 0\,\mathrm{m}, \quad \Delta \varphi_j = \pm 0\,rd,\ j = 1, \ldots, 7.$$

The uncertainties of the coefficients x_i and the heat transfer coefficient $h(\varphi)$ were determined using the error propagation rule formulated by Gauss.

The calculation according method I, assuming $n = 3$, $m = 7$ and $N = 30$, yielded the following results: $x_1 = 62.1773 \pm 0.6159 W/(m^2K)$, $x_2 = 59.6261 \pm 0.8315\,W/(m^2K)$, $x_3 = 47.0777 \pm 2.1291\,W/(m^2K)$. The minimum sum of squares is $= 2.6577\,K^2$. The second method gave the results: $x_1 = 109.9594 \pm 0.3849\,°C$, $x_2 = -4.4483 \pm 0.5043\,°C$, $x_3 = -0.9702 \pm 0.5261\,°C$. The minimum sum of squares is: $S = 2.7477\,K^2$. The singular values of the matrix $\boldsymbol{A}$: $s_1 = 2.6956$, $s_2 = 1.8655$, $s_3 = 1.983$ are considerably greater than zero, so the inverse heat conduction problem is well conditioned. The variation of the heat transfer coefficient $h(\varphi)$ and the wall temperature $T(r_m, \varphi)$ determined by the first method are shown in Figs. 7a and 8a, respectively. Figure 9a presents the upper and lower limit of the 95% confidence interval for $h(\varphi)$ determined by method I. Similar results are achieved using method II. It follows from Fig. 9a that the uncertainty of the determined plot of $h(\varphi)$ is moderate. Figure 9a demonstrates that the presented methods are able to determine heat transfer coefficient for actual data perturbated with errors.

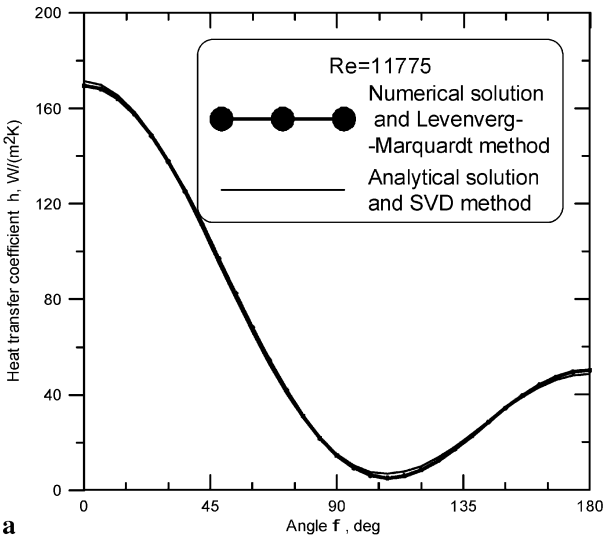

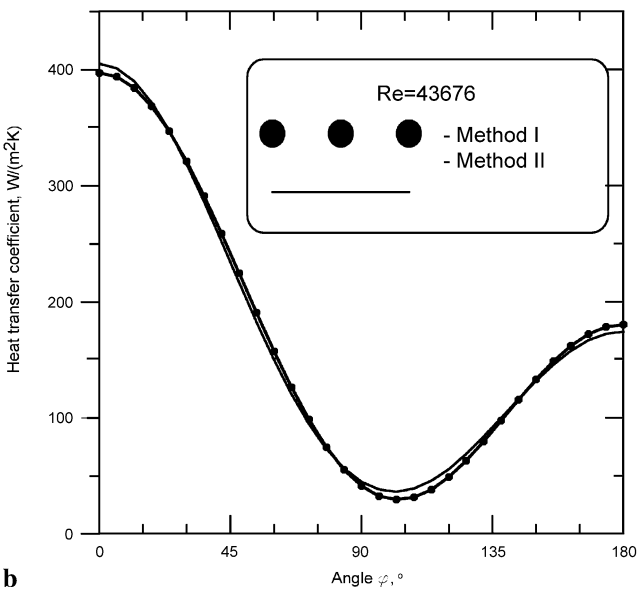

Fig. 7 Comparison of heat transfer coefficients $h(\varphi)$ on tube half circumference determined by both methods; **a** Re = 11 775, **b** Re = 43 676

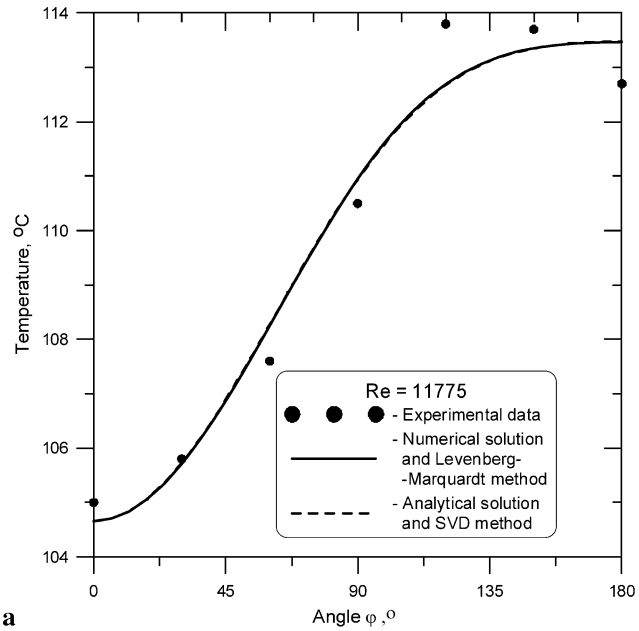

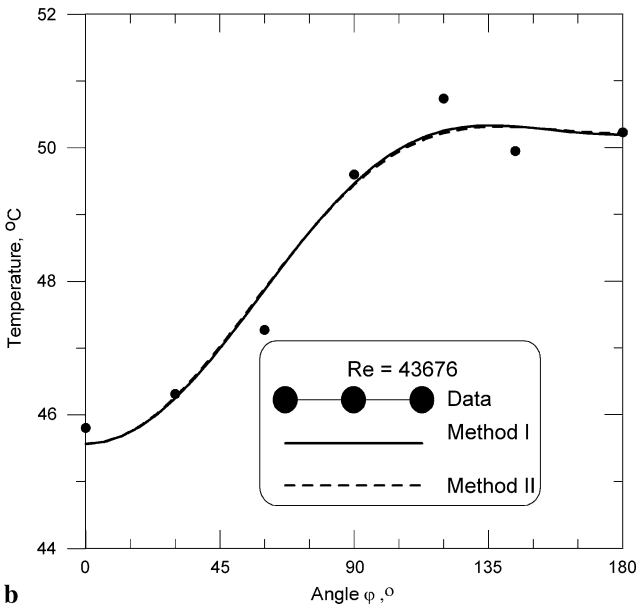

Fig. 8 Comparison of the temperatures $T(r_m, \varphi_i)$ on tube half circumference determined by both methods with measured data; **a** Re = 11 775, **b** Re = 43 676

The heat transfer coefficient was also determined for the higher Reynolds number: Re = 43 676. The following data was used for the inverse analysis: $\dot{Q}_h = 98.79\,\mathrm{W}$, $T_\infty = 22.17\,^\circ\mathrm{C}$, $f_1 = 45.8\,^\circ\mathrm{C}$, $f_2 = 46.31\,^\circ\mathrm{C}$, $f_3 = 47.27\,^\circ\mathrm{C}$, $f_4 = 49.60\,^\circ\mathrm{C}$, $f_5 = 50.74\,^\circ\mathrm{C}$, $f_6 = 49.95\,^\circ\mathrm{C}$, $f_7 = 50.23\,^\circ\mathrm{C}$.

The uncertainties of the measured values are assumed to be the same as in the previous case.

The calculation according method I, assuming $n = 3$, $m = 7$ and $N = 30$ gave the following results: $x_1 = 165.133 \pm 1.892\,\mathrm{W/(m^2K)}$, $x_2 = 108.460 \pm 2.704\,\mathrm{W/(m^2K)}$, $x_3 = 123.76 \pm 8.223\,\mathrm{W/(m^2K)}$. The minimum sum of squares is $S = 0.7952\,\mathrm{K}^2$. The second method yielded: $x_1 = 48.628 \pm 0.385\,^\circ\mathrm{C}$, $x_2 = -2.349 \pm 0.504\,^\circ\mathrm{C}$, $x_3 = -0.804 \pm 0.526\,^\circ\mathrm{C}$. The minimum sum of squares is $S = 0.8593\,\mathrm{K}^2$. The singular values of the matrix $\boldsymbol{A}$ are the same as for Re = 11 775 because the matrices $\boldsymbol{A}$ are identical in both cases. The comparison of the calculated temperature variation with the experimental data is shown in Fig. 8b. The comparison of the heat transfer distribution obtained by the both methods is depictured in Fig. 8. It is seen that both methods yield nearly the same results. A better agreement between the calculated values of $T(r_m, \varphi_i)$ and the varying temperatures can be achieved by increasing the degree of the trigonometric polynomial, e.g. to $n = 5$. In order to raise the accuracy of values $h(\varphi)$ along the tube circumference it is however indispensable to increase the number of wall temperature measuring points and at the same time to increase the degree of the trigonometric polynomial. The estimated distribution of the heat transfer coefficient on the tube semi-circumference is shown in Fig. 9b.

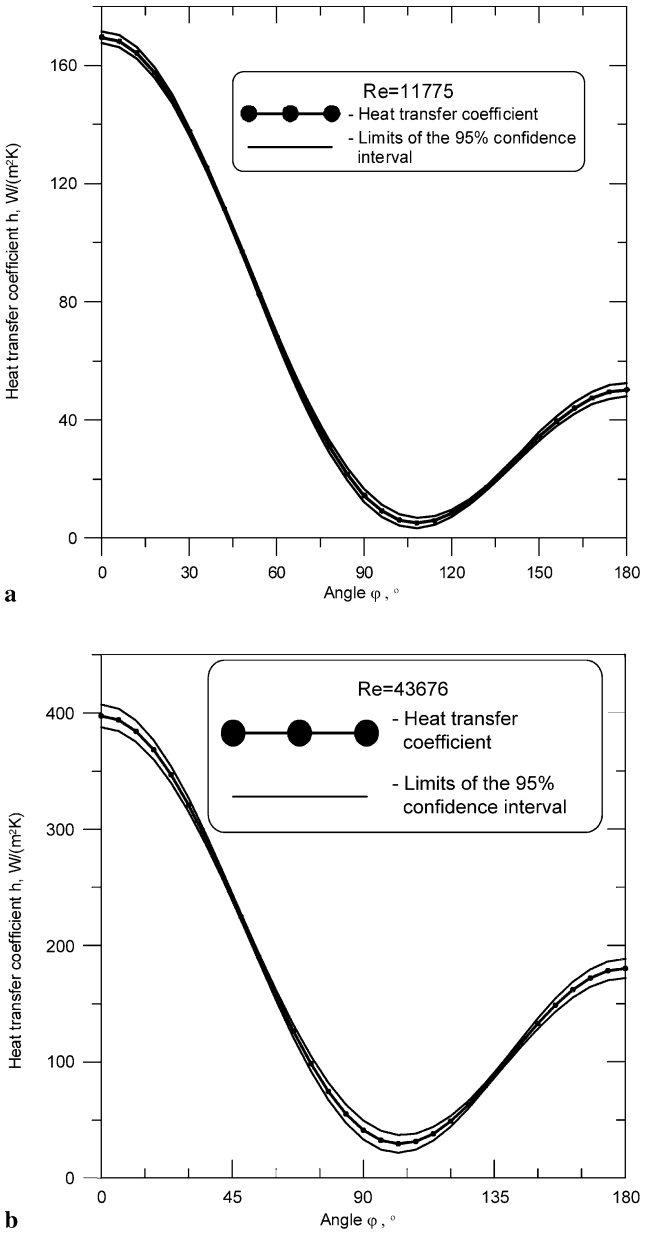

Fig. 9 Heat-transfer coefficient values on tube half circumference determined by method I and the 95% confidence interval; **a** Re = 11 775, **b** Re = 43 676

7 Conclusions

Comparing both methods to determine the values of the heat transfer coefficient on the tube circumference presented in this paper leads to the conclusion that both methods yield very similar results. The first one, based on numerical iterative determination of the temperature field and solving the non-liner inverse problem by the Levenberg–Marquardt scheme is more universal, but the computing time is longer.

When the number of unknown parameters is greater, then it is difficult to select the parameter start values, which assure the convergence of the iteration process.

In the second method, the distribution of temperature is determined analytically and the over-determined set of algebraic equations is solved by decomposition of the matrix of coefficients according to singular values. The computation time needed by the second method is very short.

Both methods are suitable to solve ill conditioned inverse problems of heat transfer. Upon minor modifications they can also be used to determine the heat transfer coefficient on the surface of tubes with the heat thermal conductivity dependent on temperature.

References

1. Saboya FE, Sparrow EM (1974) Local and average transfer coefficients for one-row plate fin and tube heat exchanger configurations. J Heat Transf 96:265–272
2. Goldstein RJ, Cho HH (1995) A review of mass transfer measurements using naphthalene sublimation. Exp Therm Fluid Sci 10:416–434

3. Kottke V, Geschwind P, Li HD (1997) Heat and mass transfer along curved walls in internal flows. ERCOFTAC Bull 32: 21–24
4. Krückels SW, Kottke V (1970) Investigation of the distribution of heat transfer on fins and finned tube models. Chem Eng Technol 42:355–362
5. Baughn JW, Mayhew JE, Anderson MR, Butler RJ (1998) A periodic transient method using liquid crystals for the measurement of local heat transfer coefficients. J Heat Transf 119:242–248
6. Wang Z, Ireland PT, Jones TV, Davenport R (1996) A color image processing system for transient liquid crystal heat transfer experiments. J Turbomach 118:421–427
7. Smits AJ, Lim TT (Eds) (2003) Flow Visualization: Techniques and Examples. Imperial College Press, Singapore
8. Ervin J, Bizzak DJ, Murawski C, Chyu MK, MacArtur C (1993) Surface temperature determination of a cylinder in cross flow with thermographic phosphors, Visualization of Heat Transfer Processes, HTD-Vol 252. The American Society of Mechanical Engineers, New York
9. Merski NR (1999) Global aeroheating wind-tunnel measurements using improved two-color phosphor thermography method. J Spacecr Rockets 36:160–170
10. Liu T, Sullivan JP (2005) Pressure and Temperature Sensitive Paints. Springer, Berlin
11. Mayinger F (1993) Image-forming optical techniques in heat transfer: revival by computer aided data processing. J Heat Transf 115:824–834
12. Naylor D (2003) Recent developments in the measurement of convective heat transfer rates by laser interferometry. Int J Heat Fluid Flow 24:345–355
13. Giedt WH (1949) Investigation of variation of point unit-heat-transfer coefficient around a cylinder normal to an air stream. Trans ASME 71:375–381
14. Sanitjai S, Goldstein R (2004) Forced convection heat transfer from a circular cylinder in cross-flow to air and liquids. Int J Heat Mass Transf 47:4795–4805
15. Taler J (1992) Numerical solutions for general inverse heat conduction problem. Wärme- Stoffübertrag 27:505–513
16. Taler J (2001) Inverse determination of local heat transfer coefficients. Trans Inst Fluid Flow Mach 109:87–100
17. Taler J, Sobota T, Cebula A (2005) Determining spatial distribution of the heat transfer coefficient on the surface of complex shape. Arch Thermodyn 26(1):35–52
18. Kikuchi Y, Suzuki H, Kitagawa M, Ikeya K (2000) Effect of pulsating Strouhal number on heat transfer around a heated cylinder in pulsating cross-flow. JSME Int J B 43(2):250–257
19. Taler J, Duda P (2006) Solving Direct and Inverse Heat Conduction Problems. Springer, Berlin
20. Seber GAF, Wild CJ (1989) Nonlinear Regression. John Wiley & Sons, New York
21. Golub GH, Van Loan CF (1989) Matrix Computations, 2nd Edition. John Hopkins University Press, Baltimore
22. (2000) Policy on Reporting Uncertainties in Experimental Measurements and Results. Trans ASME J Heat Transf 122:411–413